Preprints (www.preprints.org) | NOT PEER-REVIEWED | Posted: 24 March 2017 doi:10.20944/preprints201703.0187.v1

Article

Fatigue Life Estimation of Medium-Carbon Steel with Different Surface Roughness

Changyou Li *, Weibing Dai, Fei Duan, Yimin Zhang, and David He

School of Mechanical Engineering and Automation, Northeastern University, Shenyang 110819, China; yifanwb@163.com (W.D.); ymzhang@sohu.com (Y.Z.); davidhe@uic.edu (D.H.)

* Correspondence: chyli@mail.neu.edu.cn

Abstract: Medium-carbon steel is commonly used for the rail, wire ropes, tire cord, cold heading, forging steels, cold finished steel bars, machinable steel and so on. Its fatigue behavior analysis and fatigue life estimation play an important role in the machinery industry. In this paper, the estimation of fatigue life of medium-carbon steel with different surface roughness using established S-N and P-S-N curves is presented. To estimate the fatigue life, the effect of the average surface roughness on the fatigue life of medium-carbon steel has been investigated using 75 fatigue tests in three groups with average surface roughness (R_a): 0.4μm, 0.8μm, and 1.6μm respectively. S-N curves and P-S-N curves have been established based on the fatigue tests. The fatigue life of medium-carbon steel is then estimated based on Tanaka-Mura crack initiation life model, the crack propagation life model using Paris law, and material constants of the S-N curves. 6 more fatigue tests have been conducted to validate the presented fatigue life estimation formulation. The experimental results have shown that the presented model could estimate well the mean fatigue life of medium-carbon steel with different surface roughness.

Key words: medium-carbon steel; fatigue life estimation; surface roughness

1. Introduction

Medium-carbon steel is usually referred as to the carbon steel that contains approximately 0.30 – 0.60% carbon element content. It balances ductility and strength, and has good wear resistance [1]. It is commonly used for the rail, wire ropes, tire cord, cold heading, forging steels, cold finished steel bars, machinable steel and so on [2]. Its fatigue behavior analysis and fatigue life estimation play an important role in the safety and reliability in the machinery industry. From a raw steel piece to a part meeting the design requirements, a manufacturing process must be used. The surface roughness of a part as a result of the manufacturing process plays a major role in determining the fatigue behavior of the part [3]. To ensure the high safety and reliability of the part of medium-carbon steel in service, it is important to investigate S-N curve, P-S-N curve, and fatigue life of medium-carbon steel with different surface roughness.

A method has been reported where the effect of the surface roughness on fatigue behavior was commonly considered by using surface condition modification factor $k_a = aS_{ut}^b$, where S_{ut} is the minimum tensile strength, a and b are statistical values and determined by the material and the machining method such as ground, machined or cold-drawn, hot-rolled, and as-forged [4]. Then, the endurance limit S_e at the critical location of a machine part in the geometry and condition of use is proportional to the product of k_a and S_e', $S_e \propto k_a S_e'$ where S_e' is the rotary-beam test specimen endurance limit. However, it is very difficult for this method to estimate the fatigue life of the given material with the different surface roughness. Then, other methods have been proposed. For example, the surface groove due to the manufacturing process was considered to result in stress concentration similar to a notch. The fatigue stress concentration factor K_f was used for describing the effect of the surface roughness on the fatigue limit. It was the function of the stress concentration factor K_t which can be estimated by the finite element method [5, 6] or the empirical formula including

 doi:10.20944/preprints201703.0187.v1

the average geometric parameters of surface roughness [7, 8]. A method has been also reported to estimate the fatigue life by $N_f = N_i + N_p$ where N_f, N_i, and N_p were fatigue life, crack initiation life, and crack propagation life, respectively. The fatigue life can be computed as: $N_i = \beta(K_t\sigma)^{\alpha}$ where β and α are determined by plotting N_i as a function of the stress amplitude S. The crack propagation life could be estimated by iterative numerical integration of Paris law where the surface fatigue crack propagation threshold is multiplied by K_t and the fatigue crack propagation threshold in depth is not affected [5]. For the large surface roughness, the stress concentration due to the surface groove might be obvious and the methods of estimating the fatigue life based on the stress concentration factor might have the high accuracy. However, the stress concentration factor might be very close to 1 for small surface roughness. Moreover, accurately computing the stress concentration factor is a time-consuming and complex process. Therefore, the method has been reported where the surface groove due to machining was considered to be an initial micro-defect. The analytic formulation of the crack initiation life N_i can be estimated based on the dislocation dipole accumulation model [9-11] and the crack propagation life N_p can calculated using the analytic solution of Paris law integral [12-14]. Since the reported method has been validated by six types of the ultra-high strength steel [11] and the high strength martensitic stainless steel [12], it will be employed to estimate the fatigue life of medium-carbon steel with the different surface roughness in this paper.

The remainder of this paper is organized as follows: In Section 2, the material, the specimen geometry, and the testing apparatus will be described, the scatter plot of the fatigue experiment results shown, and the mean fatigue life of the specimens with different average surface roughness contrasted. In Section 3, S-N and P-S-N curves will be established and their curve fitting parameters listed. In Section 4, the formulation for estimating the mean fatigue life of medium-carbon steel with different average surface roughness will be explained along with its validation. The conclusions are drawn finally in Section 5.

2. Material and Experimental Results

2.1 Material and testing apparatus

The material investigated in this work is the medium-carbon steel and its composition is presented in Table 1. The raw material is a hot rolled steel bar and is machined into the funnel specimen. The geometry of the specimen is shown in Fig. 1. The specimens were polished to the specified average surface roughness. To investigate the effect of the different surface roughness of the specimens on the fatigue life, specimens were machined into three groups with average surface roughness (R_a) : 0.4μm, 0.8μm, and 1.6μm, respectively. The rotating bending fatigue tests were performed. The testing apparatus is shown in Fig. 2. The cycle frequency was 25Hz.

Table 1. Chemical composition of the medium-carbon steel

Element	C	Cr	Mo	Si	Mn	S	P	Ni
Weight (%)	0.44	0.04	0.02	0.23	0.57	0.016	0.024	0.002

Preprints (www.preprints.org) | NOT PEER-REVIEWED | Posted: 24 March 2017 doi:10.20944/preprints201703.0187.v1

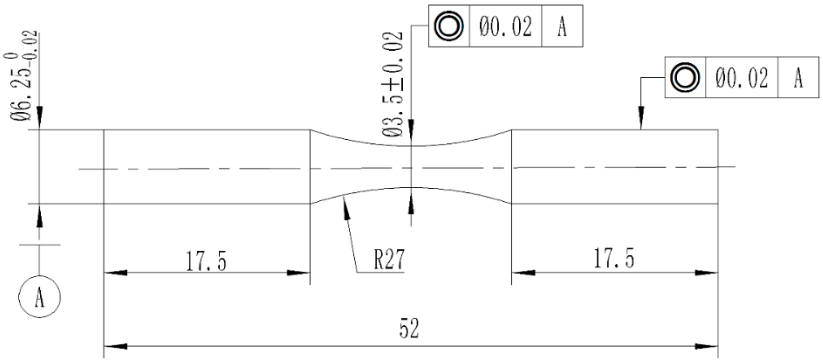

Fig. 1 Fatigue specimen geometry (dimensions in mm)

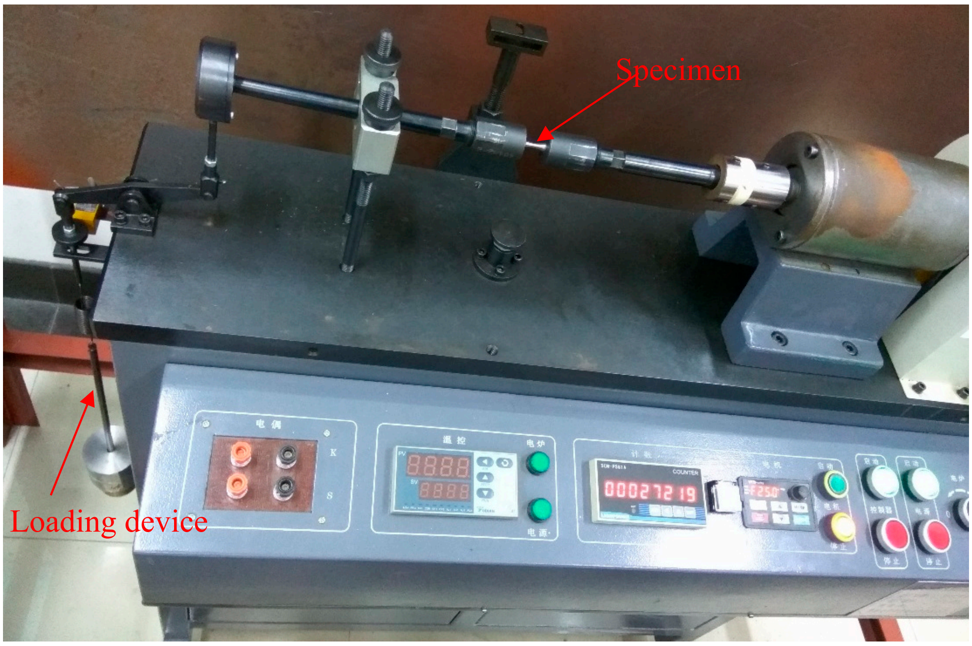

Fig. 2 The testing apparatus

2.2 Experimental results

In this work, 75 fatigue tests were conducted. They were divided into three groups with average surface roughness (R_a) of 0.4μm, 0.8μm, and 1.6μm, respectively. The stress amplitudes of the first group (R_a=0.4μm) included 550, 500, 450, 400, and 380MPa and those of other two groups included 500, 450, 400, 380, and 360MPa. A total of 5 fatigue tests were performed under each stress amplitude. The scatter plot of all the experimental results is shown in Fig. 3. Under each stress amplitude, it can be seen that the fatigue life has the conspicuous dispersion. The means of fatigue life with different average surface roughness and stress amplitude are compared in Fig. 4. The average surface roughness is clearly effective in reducing mean of fatigue life for medium-carbon steel. In high stress amplitude (for example 500MPa), there is about 15% decrease while there is about 30% decrease in low stress amplitude (for example 380MPa) when the average surface roughness increased from 0.4μm to 0.8μm or from 0.8μm to 1.6μm. This could confirm that the surface roughness plays a vital role in the fatigue life of medium-carbon steel.

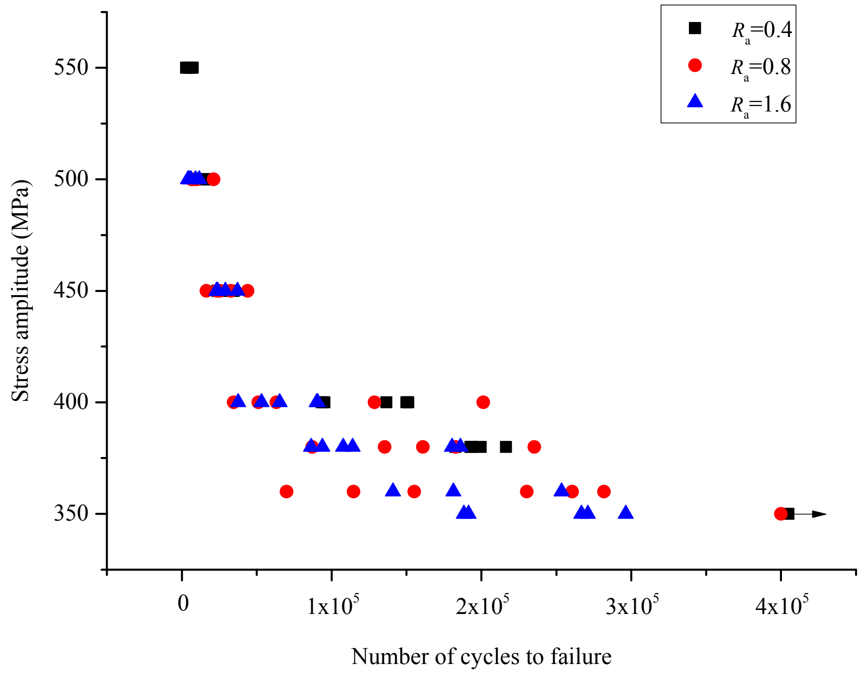

Fig. 3 Scatter plot of the 75 fatigue tests

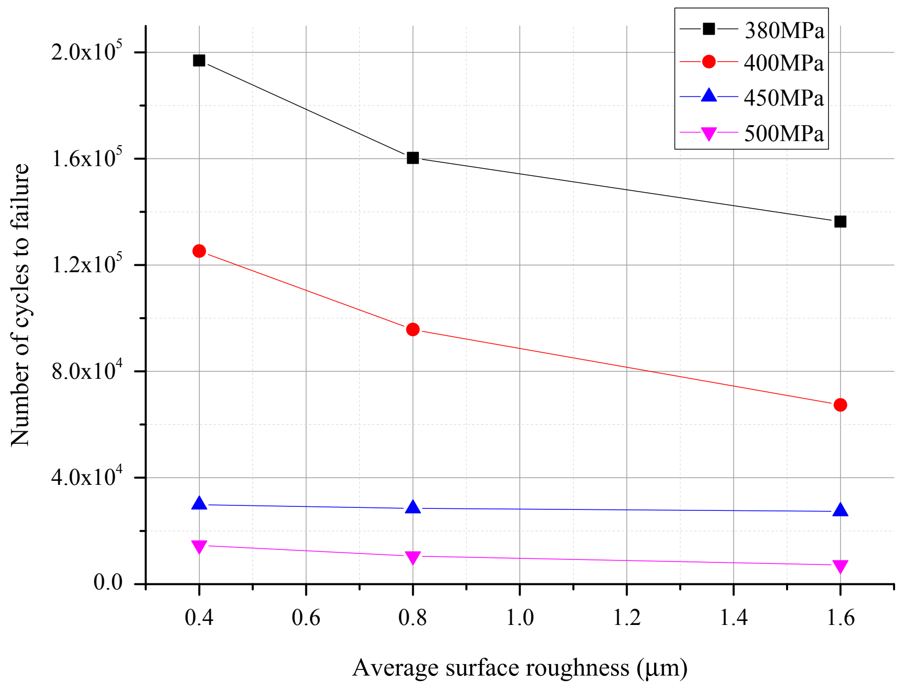

Fig. 4 Contrast of mean fatigue life with R_a=0.4μm, R_a=0.8μm, and R_a=1.6μm

Preprints (www.preprints.org) | NOT PEER-REVIEWED | Posted: 24 March 2017 doi:10.20944/preprints201703.0187.v1

3. S-N curves and P-S-N curves

The S-N curves with the different average surface roughness are shown in Fig. 5. The input data points of the curve fitting were obtained by taking the logarithm of the means of the fatigue life data and stress amplitudes. The material constants were estimated by the least square method and are listed in Table 2. The material constants satisfy the logarithmic Basquin equation $\lg N = \lg c - n \lg S$, where N is the number of cycles to failure and S is the stress amplitude.

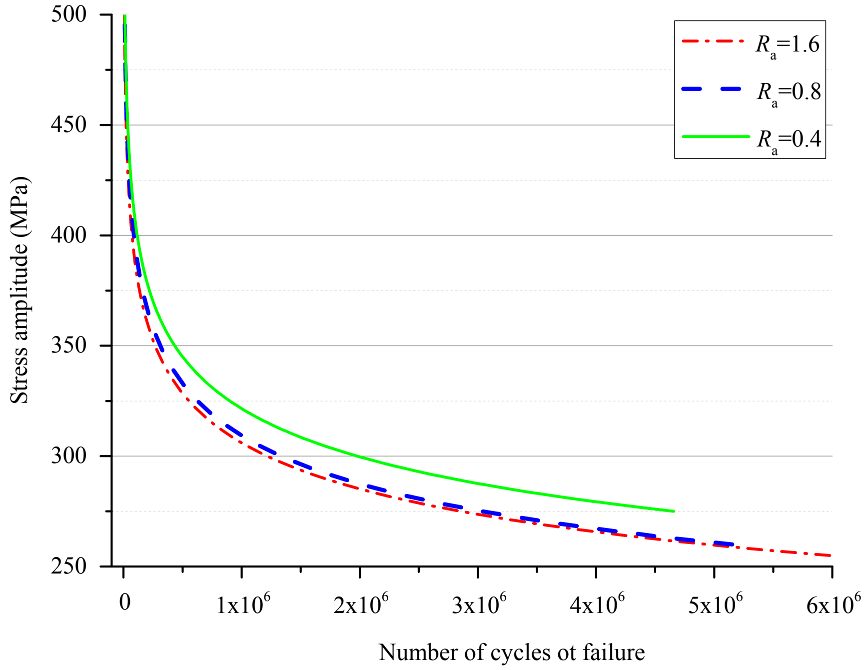

Fig. 5 The S-N curves with R_a=0.4μm, R_a=0.8μm, and R_a=1.6μm

Table 2. Material constants with the different average surface roughness

Average surface roughness	n	c
R_a=0.4μm	9.84	4.56×10^{30}
R_a=0.8μm	9.44	3.16×10^{29}
R_a=1.6μm	9.80	2.32×10^{30}

The P-S-N curves with R_a=0.4μm, R_a=0.8μm, and R_a=1.6μm are shown in Fig. 6, 7, and 8 respectively. R is the survival probability. The data point (pink inverted triangle, blue triangle, red dot and black square) is the confidence lower limit which is calculated by [13]:

$$x_{RL} = \bar{x} + h\sigma_x \tag{1}$$

where $\bar{x}$ and σ_x are the mean and the standard deviation of the experimental fatigue life, h is the one-sided tolerance factor which is calculated by:

$$h = u_R\beta - t_\gamma\sqrt{\frac{1}{n} + u_R^2\left(\beta^2 - 1\right)} \tag{2}$$

In Eq. (2), u_R=$\Phi^{-1}(R)$, $\Phi^{-1}(\bullet)$ is the inverse function of the standard normal distribution function, β the correction factor, t_γ=$\mathrm{T}^{-1}(\gamma)$, $\mathrm{T}^{-1}(\bullet)$ the inverse function of the distribution function of Student's t-distribution with n–1 degrees of freedom, and n the sample size. When the

Preprints (www.preprints.org) | NOT PEER-REVIEWED | Posted: 24 March 2017 doi:10.20944/preprints201703.0187.v1

survival probability R and the confidence level γ are given, the confidence lower limit can be calculated by Eq. (1). Then, P-S-N curve is described by the similar logarithmic Basquin equation $\lg N = a - b \lg S$, where parameters a and b are estimated by the least square method with R_a=0.4μm, R_a=0.8μm, and R_a=1.6μm shown in Table 3, 4, and 5 respectively.

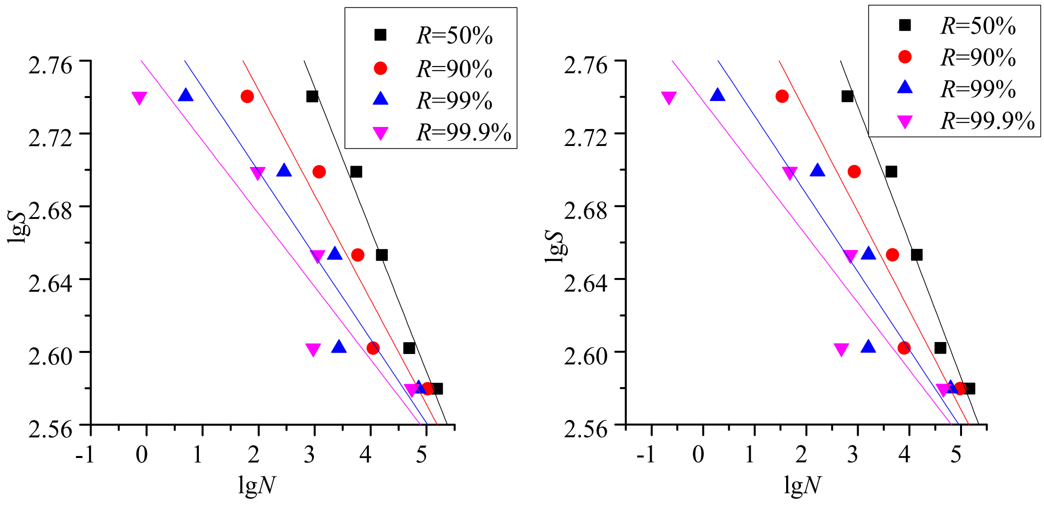

(a) (b)

Fig. 6 The P-S-N curves with R_a=0.4μm and confidence level (a) γ=95%, (b) γ=99%

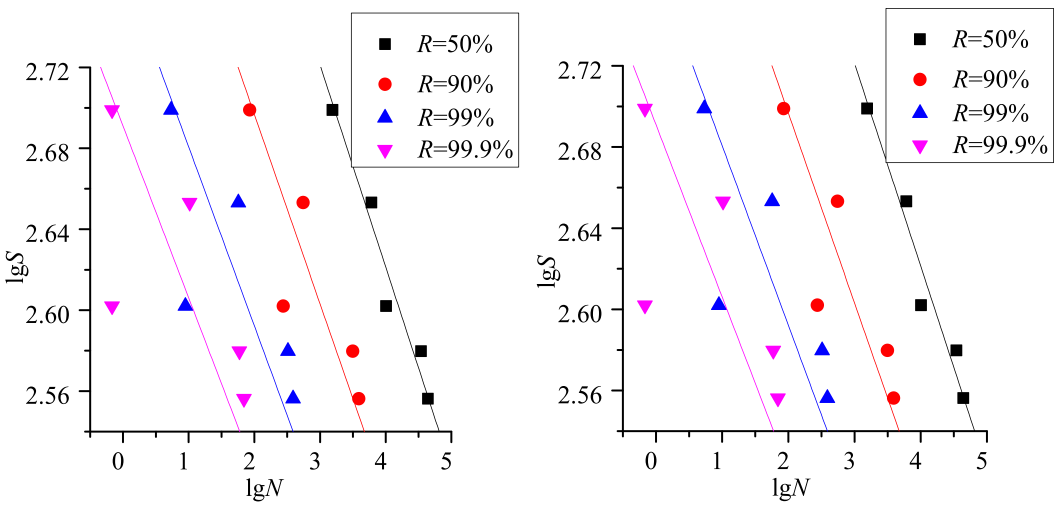

Fig. 7 The P-S-N curves with R_a=0.8μm and confidence level (a) γ=95%, (b) γ=99%

 doi:10.20944/preprints201703.0187.v1

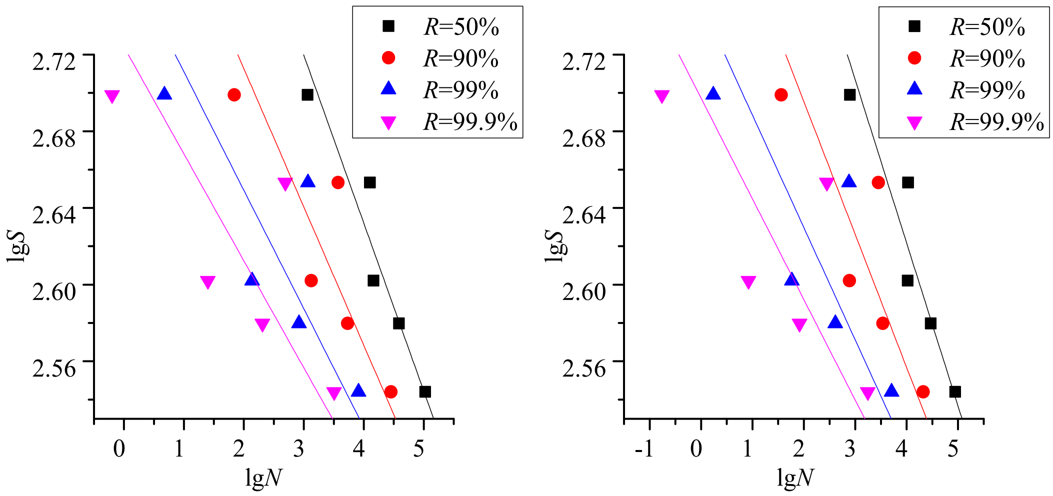

Fig. 8 The P-S-N curves with R_a=1.6μm and confidence level (a) γ=95% , (b) γ=99%

Table 3. Parameters of P-S-N curves with R_a=0.4μm

γ (%) \ R (%)	50	90	99	99.9	Parameters
95	40.7137	54.1796	66.9757	76.5668	*a*
	-13.9865	-19.3591	-24.4740	-28.3078	*b*
99	42.5752	57.2561	71.7960	82.7595	*a*
	-14.7206	-20.5889	-26.4008	-30.7832	*b*

Table 4. Parameters of P-S-N with R_a=0.8μm

γ (%) \ R (%)	50	90	99	99.9	Parameters
95	28.6827	29.3268	29.9388	30.3976	*a*
	-9.4241	-10.1261	-10.7931	-11.2931	*b*
99	28.7717	29.4739	30.1694	30.6938	*a*
	-9.5212	-10.2864	-11.0444	-11.6159	*b*

Table 5. Parameters of P-S-N curves with R_a=1.6μm

γ (%) \ R (%)	50	90	99	99.9	Parameters
95	34.0511	39.5910	44.8554	48.8012	*a*
	-11.4174	-13.8578	-16.1769	-17.9151	*b*
99	34.8170	40.8567	46.8385	51.3489	*a*
	-11.7547	-14.4154	-17.0504	-19.0374	*b*

Preprints (www.preprints.org) | NOT PEER-REVIEWED | Posted: 24 March 2017 doi:10.20944/preprints201703.0187.v1

4. Fatigue Life Estimation

The fatigue life N_f is composed of the crack initiation life N_i and the crack propagation life N_p and can be expressed as:

$$N_f = N_i + N_p \tag{3}$$

The analytic formulation of the crack initiation life N_i was presented by Tanaka and Mura [9-10] and was based on the dislocation dipole accumulation model. It was extended to estimate the crack initiation life N_i of the specimen with the different surface roughness by Wang *et al*. [12]. It is [9-12]:

$$N_i = \frac{9\Delta K_{th}^2 G}{E(S - S_e)^2 \pi (1-\upsilon) a_0} \tag{4}$$

where ΔK_{th} is the threshold of stress intensity factor, G the shear modulus, E elastic modulus, S_e the endurance limit, υ the Poisson's ratio, and a_0 the equivalent initial micro-defect size. a_0 could be estimated as [12, 14]:

$$a_0 = 2.97R_{\mathrm{a}} \tag{5}$$

The number of cycles necessary to grow the crack from the initial micro-defect size to failure can be described by Paris law as:

$$\frac{da}{dN} = C(\Delta K)^n \tag{6}$$

where ΔK is the amplitude of stress intensity factor, C the material constant, and a the crack size. The crack propagation life N_p can be calculated by the analytic solution of Paris law integral as [12, 15-16]:

$$N_p = \frac{a_0^{\left(1-\frac{n}{2}\right)} - a_{\mathrm{sc}}^{\left(1-\frac{n}{2}\right)}}{CS^n \beta_1^n \pi^{\frac{n}{2}}\left(\frac{n}{2}-1\right)} + \frac{a_{\mathrm{sc}}^{\left(1-\frac{n}{2}\right)} - a_{\mathrm{f}}^{\left(1-\frac{n}{2}\right)}}{CS^n \beta_2^n \pi^{\frac{n}{2}}\left(\frac{n}{2}-1\right)} \tag{7}$$

where: a_{sc} is the critical crack size for identifying long and short cracks, a_f the crack size of final failure, $\beta_1 = 0.5\sqrt{\pi}$ and $\beta_2 = 1$. Generally, the number of crack growth cycles from a_0 to a_{sc} is much greater than the cycles needed to grow from a_{sc} to a_f. Then N_p can be taken as [17]:

$$N_p = \frac{a_0^{\left(1-\frac{n}{2}\right)}}{CS^n \beta_1^n \pi^{\frac{n}{2}}\left(\frac{n}{2}-1\right)} \tag{8}$$

It can be written by:

$$S^n N_p = c \tag{9}$$

where

$$c = \frac{a_0^{\left(1-\frac{n}{2}\right)}}{C\beta_1^n \pi^{\frac{n}{2}}\left(\frac{n}{2}-1\right)} \tag{10}$$

By taking logarithms in Eq. (9), then:

$$\lg N_p = \lg c - n \lg S \tag{11}$$

Preprints (www.preprints.org) | NOT PEER-REVIEWED | Posted: 24 March 2017 doi:10.20944/preprints201703.0187.v1

The material constant n in Eq. (9) is the same as n in S-N curves. The material constant C can be solved by Eq. (10). The estimation of n and c will be discussed in Section 3. The material constants C and n in Eq. (8) are listed in Table 6.

Table 6. Material constants C and n in Eq. (5) with different average surface roughness

average surface roughness	n	C
R_a=0.4μm	9.84	4.11×10^{-34}
R_a=0.8μm	9.44	4.81×10^{-34}
R_a=1.6μm	9.80	3.02×10^{-36}

Then, the fatigue life N_f of medium-carbon steel is computed as:

$$N_f = \frac{9\Delta K_{th}^2 G}{E(S-S_0)^2 \pi(1-\nu)a_0} + \frac{a_0^{\left(1-\frac{n}{2}\right)}}{CS^n \beta_1^n \pi^{\frac{n}{2}}\left(\frac{n}{2}-1\right)} \tag{12}$$

where the shear modulus G is 79.40GPa, the elastic modulus E is 206.00GPa, and the threshold of stress intensity factor ΔK_{th} is 6.26. Substituting the material constants C and n in Table 6 into Eq. (12), the mean fatigue life N_f of medium-carbon steel with different average surface roughness is

$$N_f = \begin{cases} \dfrac{9\times6.26^2\times79.4}{206\times(S-275)^2\times\pi\times(1-0.27)\times1.188\times10^{-3}} \\ +\dfrac{1.188^{\left(1-\frac{9.835}{2}\right)}}{4.11\times10^{-34}\times S^{9.835}\times\left(0.5\sqrt{\pi}\right)^{9.835}\pi^{\frac{9.835}{2}}\left(\dfrac{9.835}{2}-1\right)} \Leftrightarrow \mathrm{Ra}=0.4 \\ \dfrac{9\times6.26^2\times79.4}{206\times(S-260)^2\times\pi\times(1-0.27)\times2.376\times10^{-3}} \\ +\dfrac{2.376^{\left(1-\frac{9.436}{2}\right)}}{4.81\times10^{-34}\times S^{9.436}\times\left(0.5\sqrt{\pi}\right)^{9.436}\pi^{\frac{9.436}{2}}\left(\dfrac{9.436}{2}-1\right)} \Leftrightarrow \mathrm{Ra}=0.8 \\ \dfrac{9\times6.26^2\times79.4}{206\times(S-255)^2\times\pi\times(1-0.27)\times4.752\times10^{-3}} \\ +\dfrac{4.752^{\left(1-\frac{9.802}{2}\right)}}{3.02\times10^{-36}\times S^{9.802}\times\left(0.5\sqrt{\pi}\right)^{9.802}\pi^{\frac{9.802}{2}}\left(\dfrac{9.802}{2}-1\right)} \Leftrightarrow \mathrm{Ra}=1.6 \end{cases} \tag{13}$$

When the average surface roughness is 0.4, 0.8, and 1.6 respectively, the mean fatigue life curves of medium-carbon steel calculated by Eq. (13) are shown in Fig. 8. It can be seen that the fatigue life estimation model agrees with the experiment value well. To validate the presented formulation for estimating the mean fatigue life of medium-carbon steel, 6 more fatigue tests were conducted and the experimental results are shown in Table 7. The stress amplitude was 420MPa and was not equal to any stress amplitude in the previous experiments. The maximum and minimum estimation errors are 15.83% and 1.99%, respectively. Therefore, it is obvious that the presented model for estimating the mean fatigue life of medium-carbon steel gives good results for roughness R_a=0.4μm, R_a=0.8μm, and R_a=1.6μm.

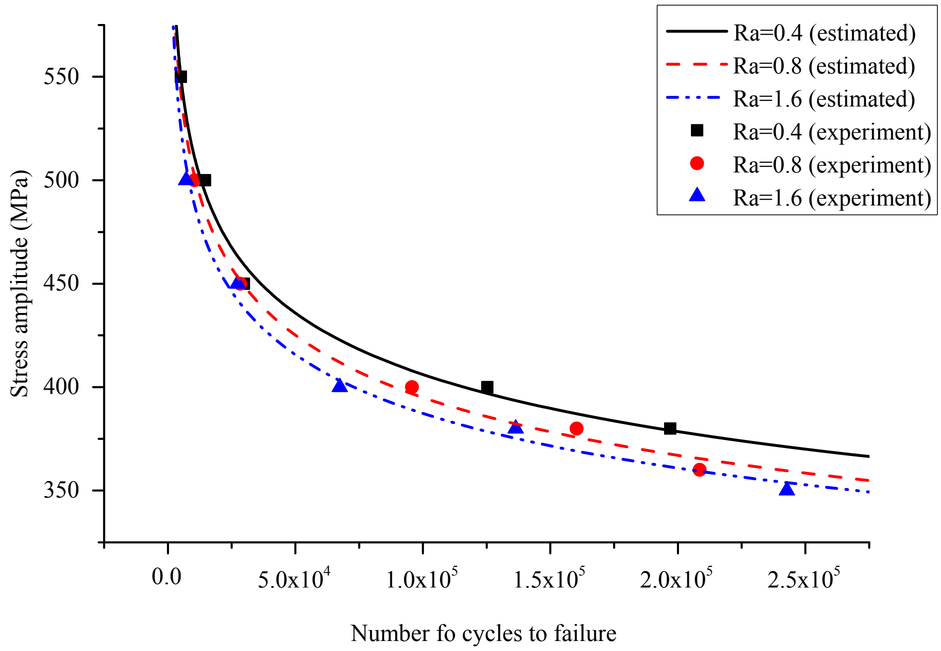

Fig. 9 Estimated mean fatigue life curves and the experiment values

Table 7. Validation experiment results

Average surface roughness	Stress amplitude	Estimated fatigue life	Experimental fatigue life	Mean of experimental fatigue life	Error
R_a=0.4μm	420MPa	72420	70569	73863	1.99%
			77156		
R_a=0.8μm		56060	57824	51120	8.81%
			44416		
R_a=1.6μm		45190	66174	52345	15.83%
			38516		

5. Conclusions

To estimate the fatigue life of medium-carbon steel sample, the effect of the average surface roughness on the fatigue life has been investigated in this paper using 75 fatigue tests in three groups with average surface roughness (Ra): 0.4μm, 0.8μm, and 1.6μm respectively. In high stress amplitude (for example 500MPa), there is about 15% decrease of the mean fatigue life while there is about 30% decrease in low stress amplitude (for example 380MPa) when the average surface roughness increased from 0.4μm to 0.8μm or from 0.8μm to 1.6μm. Then, one new method was presented to estimate the fatigue life of the medium-carbon steel with different average surface roughness (R_a). The experiment results show that the maximum estimation error of the mean fatigue life by the presented model is less than 16%.

Acknowledgements: The work is supported by National Natural Science Foundation of China (Grant No. 51575095, 51675089), and Major State Basic Research Development Program of China (973 Program) (Grant No. 2014CB046303).

References

1. The Wikipedia page on carbon steel: https://en.wikipedia.org/wiki/Carbon_steel#cite_note-10 or the engineering fundamentals page on medium-carbon steel: http://www.efunda.com/materials/alloys/carbon_steels/medium_carbon.cfm
2. Gladman, T. Medium/High Carbon Steels for Rails, Rods, Bars and Forgings. In *Materials Science and Technology*; John Wiley & Sons, Inc: Hoboken, USA, 2006; pp. 401-432
3. Moussaoui, K.; Mousseigne, M.; Senatore, J.; Chieragatti, R. The effect of roughness and residual stresses on fatigue life time of an alloy of titanium. *Int. J. Adv. Manuf. Technol.* 2015, 78, 557–563, DOI: 10.1007/s00170-014-6596-7. Available online: 10 December 2014
4. Budynas, R.G.; Nisbett J.K. *Shigley's Mechanical Engineering Design*, 10th ed.; McGraw-Hill Education: New York, USA, 2015; pp: 294-301.
5. Suraratchai, M.; Limido, J.; Mabru, C.; Chieragatti, R. Modelling the influence of machined surface roughness on the fatigue life of aluminum alloy. *Int. J. Fatigue* 2008, 30, 2119–2126, DOI:10.1016/j.ijfatigue.2008.06.003. Available online: 28 June 2008
6. As, S.K.; Skallerud, B.; Tveiten, B.W.; Holme, B. Fatigue life prediction of machined components using finite element analysis of surface topography. *Int. J. Fatigue* 2005, 27, 1590–1596, DOI:10.1016/j.ijfatigue.2005.07.031. Available online: 2 September 2005
7. Arola, D.; Ramulu, M. An examination of the effects from surface texture on the strength of fiber-reinforced plastics. *J. Compos Mater.* 1999, 33, 102-123, DOI: 10.1177/002199839903300201. Available online: 24 November 1997.
8. Arola, D.; Williams, C.L. Estimating the fatigue stress concentration factor of machined surfaces. *Int. J. Fatigue* 2002, 24, 923-930, Identifier: http://dx.doi.org/10.1016/S0142-1123(02)00012-9. Available online: 12 February 2002
9. Tanaka, K.; Mura, T. A dislocation model for fatigue crack initiation. *Int. J. Appl. Mech.* 1981, 48, 97-103, DOI: 10.1115/1.3157599.
10. Tanaka, K.; Mura, T. A theory of fatigue crack initiation at inclusions. Metall. Mater. Trans. A-Phys. Metall. Mater. Sci. 1982, 13, 117-123, DOI: 10.1007/BF02642422.
11. Wang, Q.Y.; Bathias, C.; Kawagoishi, N.; Chen, Q. Effect of inclusion on subsurface crack initiation and gigacycle fatigue strength. *Int. J. Fatigue* 2002, 24, 1269–1274, Identifier: http://dx.doi.org/10.1016/S0142-1123(02)00037-3.
12. Wang, J.L.; Zhang, Y.L.; Sun, Q.C.; Liu, S.J.; Shi, B.W.; Lu, H.T. Giga-fatigue life prediction of FV520B-I with surface roughness. *Mater. Des.* 2016, 89, 1028-1034, Identifier: http://dx.doi.org/10.1016/j.matdes.2015.10.104. Available online: 20 October 2015
13. Fu, H.M.; Gao, Z.T.; Xu, R.P. A confidence lower limit of population percentile. J. Beijing Univ. Aero. Astro. 1990, 3, 1-8, DOI: 10.13700/j.bh.1001-5965.1990.03.001.
14. Murakami Y. *Metal Fatigue: Effects of Small Defects and Nonmetallic Inclusions*. Elsevier Science Ltd: Kidlington, UK, 2002; pp: 11-24.
15. Zhang, Y.L.; Wang, J.L.; Sun, Q.C.; Zhang, H.; Jiang, P.S. Fatigue life prediction of FV520B with internal inclusions. *Mater. Des.* 2015, 69, 241-246, Identifier: http://dx.doi.org/10.1016/j.matdes.2014.12.022. Available online: 30 December 2014
16. Wang, Q.Y.; Pidaparti, R.M.; Palakal, M.J. Comparative study of corrosion–fatigue in aircraft materials. *AIAA J.* 2001, 39, 325-330, DOI: 10.2514/2.1308. Available online: 11 August 2000.
17. Wang, Q.Y.; Berard, J.Y.; Rathery, S.; Bathias, C. High-cycle fatigue crack initiation and propagation behaviour of high-strength spring steel wires. *Fatigue Fract. Eng. Mater. Struct.* 1999, 22, 673-677, DOI: 10.1046/j.1460-2695.1999.t01-1-00184.x. Available online: 15 August 1999